International Journal of Mass Spectrometry 368 (2014) 23–29

Contents lists available at ScienceDirect

International Journal of Mass Spectrometry

journal homepage: www.elsevier.com/locate/ijms

Fragmentation differences in the EI spectra of three synthetic cannabinoid positional isomers: JWH-250, JWH-302, and JWH-201

Dana N. Harris[a], Stephen Hokanson[a], Vickie Miller[a], Glen P. Jackson[b,c,*]

[a] Virginia Department of Forensic Science, Commonwealth of Virginia, Roanoke, VA 24019, United States
[b] Forensic & Investigative Science, West Virginia University, Morgantown, WV 26506-6121, United States
[c] C. Eugene Bennett Department of Chemistry, West Virginia University, Morgantown, WV 26506, United States

ARTICLE INFO

Article history:
Received 8 May 2014
Accepted 9 May 2014
Available online 17 May 2014

Keywords:
Synthetic cannabinoids
Herbal spice
Ortho effect
JWH-250
JWH-302
JWH-201

ABSTRACT

The cannabinomimetic drug JWH-250 is found in herbal "spice" mixtures and is banned in many parts of the world. It is easy to misidentify JWH-250 with the positional isomers JWH-302 and JWH-201 using conventional gas chromatograph/mass spectrometry (GC/MS) because all three compounds have similar GC retention times and nearly identical mass spectra. The isomers differ by the position of a methoxy group on one of the aromatic rings; the methoxy is either *ortho*, *meta* or *para* relative to the indole substituent. Statistical analysis of principal fragment ions in the 70 eV electron ionization mass spectra of each synthetic cannabinoid showed the three isomers to be very significantly different in their respective ratios of *m*/*z* 121:91, thus forming an utilizable method for differentiation. The different abundance ratios of *m*/*z* 121:91 is explained by the ease of loosing the methoxy group when it is *ortho*, *meta* or *para* to an acetyl-indole-containing group in the different isomers. The ratios of *m*/*z* 121:91 were averaged across three different instruments over an extended period and provided *m*/*z* 121:91 ratios of: JWH-250 (*ortho* isomer) = 0.4 ± 0.02 (95% CI, *N* = 14); JWH-302 (*meta* isomer) = 1.3 ± 0.1(95% CI, *N* = 6); and JWH-201 (*para* isomer) = 7.2 ± 0.5 (95% CI, *N* = 7).

1. Introduction

As early as 2004, herbal "incense" laced with synthetic compounds were sold in Europe to recreational drug users as a marijuana mimic, and analysis of these early "spice" products found many agents including 1-pentyl-3-(1-naphthoyl)indole (JWH-018) [1]. JWH-018 is a cannabinoid CB_1 receptor agonist [2,3]. As JWH-018 and other cannabinomimetic agents were banned, spice manufacturers around the world introduced other compounds in an attempt to circumvent the law [4–7]. The trend in new synthetic cannabinoids appearing on the open market in various novelty products continues to this day [8]. In 2010–2011, 1-pentyl-3-(2-methoxyphenylacetyl)indole (JWH-250) was found to be prevalent in German spice mixtures [9,10], but a more recent study has shown a trend toward compounds that exhibit even greater binding affinities to CB_1 receptors [11,12]. JWH-250 is a CB_1 agonist [3] and is banned in most states and in many other parts of the world. The *meta*-methoxy positional isomer, 1-pentyl-3-(3-methoxyphenylacetyl)indole (JWH-302), is also a potent agonist [3] and may likely appear among the multitude of compounds used for spice products. The *para*-methoxy isomer, 1-pentyl-3-(4-methoxyphenylacetyl)indole (JWH-201), has a low affinity for the CB_1 receptor [3] so is less likely to appear in the clandestine markets, unless it is present as a synthetic impurity. The three isomers are depicted with their EI fragmentation spectra in Fig. 1. Because JWH-250, JWH-302, and JWH-201 are differentiated only by the *ortho*, *meta*, or *para* position of the methoxy group, they give MS spectra that are almost identical in most respects. However, careful analysis of the relative abundance of particular product ions can be utilized to conclusively differentiate each isomer based on its mass spectrum, but this information is strictly limited to specific law-enforcement agents [13]. The interpretation of mass spectrometric fragmentation patterns of synthetic cannabinoids is of continuing interest in forensic science [14] and bears similarities with other classes of drugs like ring-substituted amphetamines [15]. More recently, relative ion abundances were reported to help differentiate the 2,5-Dimethoxy-N-(2-methoxybenzyl)phenethylamine (NBOMe) series of designer drugs with its 3- and 4-methoxy isomers [16]. The authors noted that the abundance of the tropylium ion at *m*/*z* 91 was useful in differentiating between the different

* Corresponding author at: Department of Forensic and Investigative Science, West Virginia University, Morgantown, WV, 26506-6121, United States.
Tel.: +1 304 293 9236; fax: +1 304 293 2336.
E-mail address: glen.jackson@mail.wvu.edu (G.P. Jackson).

http://dx.doi.org/10.1016/j.ijms.2014.05.005
1387-3806/

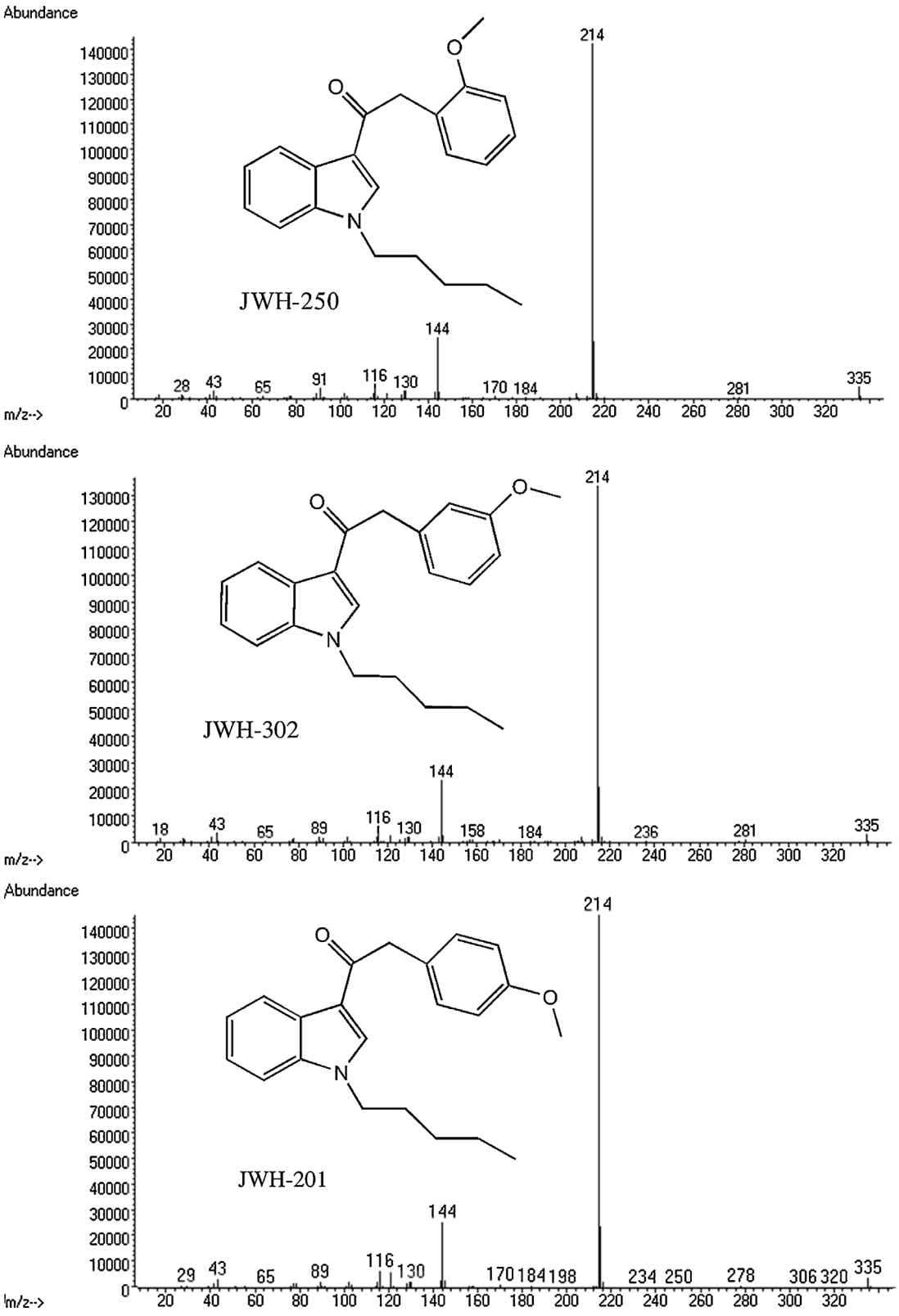

Fig. 1. EI-MS spectra of synthetic cannabinoids JWH-250, JWH-302 and JWH-201 at 70 eV electron energy.

positional isomers of the designer drug analogs, but did not specifically link the abundance of the tropylium ion to the methoxy precursor at *m*/*z* 121.

These examples show that there are likely to be many more instances where analysts may benefit from a more fundamental understanding of the ion abundances observed in EI fragmentation patterns and why certain positional isomers favor certain pathways. Although the ortho-effect described herein is generally well known to those experienced in EI interpretation, the explicit application to designer drugs presented here will hopefully help others

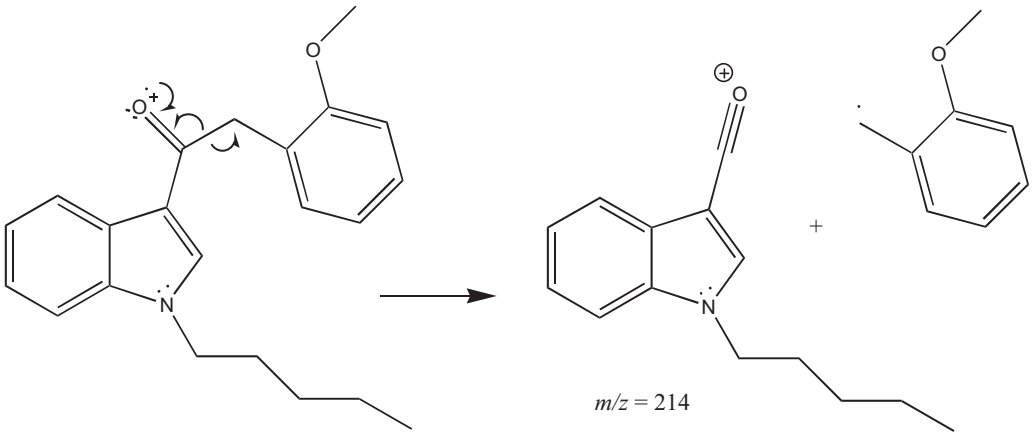

Scheme 1. Proposed scheme for formation of *m*/*z* 214 fragment (from carbonyl oxygen).

understand how to apply this understanding to the spectral interpretation of legal or scheduled compounds.

2. Experimental

Drug standards (JWH-250, JWH-302, and JWH-201) were purchased from Cayman Chemical (Ann Arbor, MI). A solution of each standard was made to an approximate concentration of 1 mg/ml in ACS solvent grade methanol from Burdick & Jackson (Morristown, NJ). Cayman Chemical supplies both JWH-302 and JWH-201 in a solution of methyl acetate. Separate aliquots were evaporated to dryness before being reconstituted in methanol.

The compounds were analyzed using three Agilent 6890 Series Gas Chromatographs each with a dual-capillary column configuration coupled to Agilent 5973 Series Mass Selective Detectors (front detectors) and flame ionization detectors (back detectors). The lead ends of both columns were situated in parallel using a double-hole ferrule attached to the front injection port. For each sample, a single injection volume of 1.0 μL was introduced into the instrument at a 40:1 split ratio. The column leading to the MSD was an HP-5ms capillary (15 m × 0.25 mm I.D., 0.25 μm film thickness) and the second column for the FID was an HP-1ms capillary (15 m × 0.25 mm I.D., 0.25 μm film thickness); both purchased from Agilent Technologies (Santa Clara, CA). Helium carrier gas flow rate was 1.8 ml/min (front column) and 1.4 ml/min (back column). The GC oven temperature began at 240 °C, held for 1 min, increased to 300 °C at 30 °C/min, and then held at 300 °C for 5 min. Mass spectra were obtained in scan mode in the range of *m*/*z* 14–500 with the electron ionization energy set at 70 eV. The MS solvent delay was set at 1.25 min. The FID used 35 ml/min hydrogen flow, 350 ml/min air flow, and 35 ml/min nitrogen makeup flow.

To assess reproducibility of mass spectral results, repeat injections were made on three separate Agilent 6890/5973 GC/MS instruments (two additional instruments were also used for JWH-250) on several different days. Samples were injected a different number of times on different days due to availability and time between caseloads. All instruments were tuned daily using perfluorotributylamine and standard autotune parameters. The results of the multiple injections were tabulated into Microsoft Excel where ion abundance ratios, mean ion abundance ratios, standard deviations, and 95% confidence intervals were calculated. Data Analysis was also performed using SPSS/PASW Statistics for Windows 18.0.

Semi-empirical and ab-initio calculations of a proposed +1 singly charged *m*/*z* 214 fragment were performed using PC based Hyperchem 6.01. The structure was optimized using AM1 with Polak-Ribiere algorithm to an RMS gradient of 0.01 kcal/[Å/mol]. Further single-point *ab-initio* calculations were performed using the 6-31G** basis set. A calculation of the charged singlet species (product of Schemes 2 and 3) was performed using restricted Hartree–Fock and a calculation of a hypothetical charged triplet (diradical) species was calculated using unrestricted Hartree–Fock.

3. Results and discussion

Retention times for the three isomers were found to be consistent on a day-to-day basis. Typical GC retention times for JWH 250, 302 and 201 on an HP-1ms column for one selected day were 3.250, 3.327 and 3.487 min, respectively. On an HP-5ms column, the compounds eluted in the same order with retention times of 3.156,

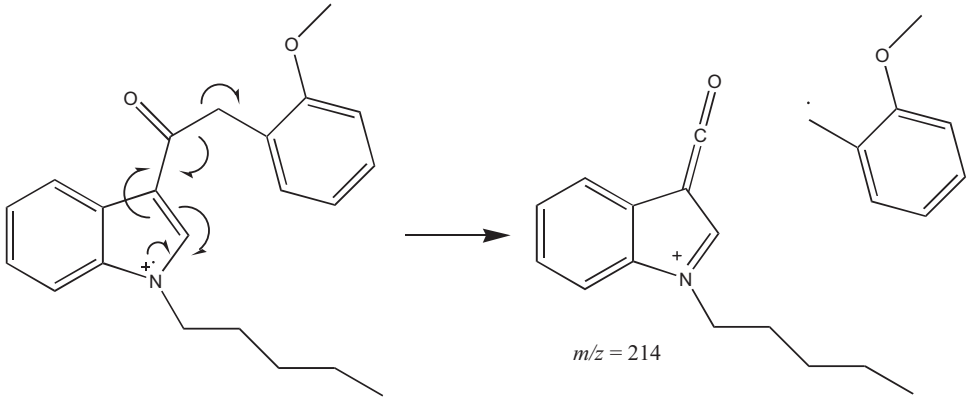

Scheme 2. Proposed scheme for the formation of *m*/*z* 214 fragment (from nitrogen).

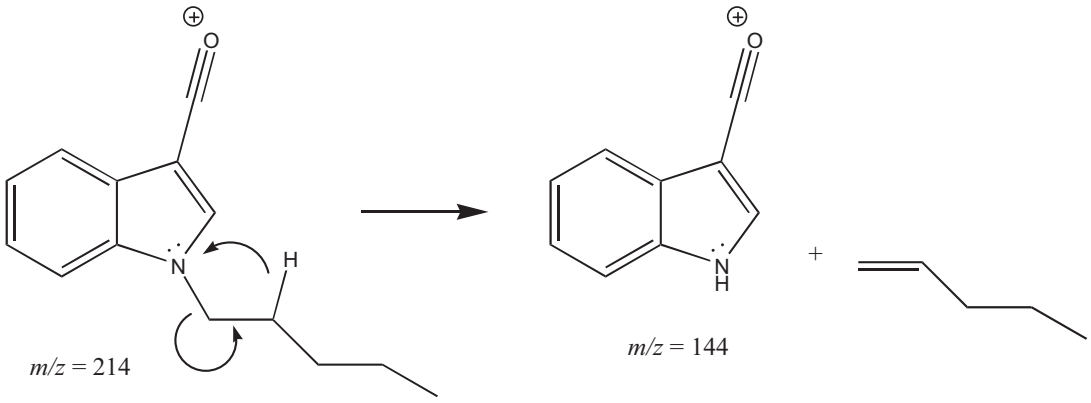

Scheme 3. Proposed mechanism for *m*/*z* 144 fragment via 1,3 hydride transfer.

3.241 and 3.393 min, respectively. Whereas the absolute retention times were different for the three isomers on the different stationary phases, the selectivity—as reflected by the relative retention times—was not significantly different between the two columns. For both HP-1ms and HP-5ms columns, the difference in GC retention times between JWH-250 and JWH-302 was typically 4–5 s and the difference between JWH-302 and JWH-201 was typically 9–10 s. Therefore, the two stationary phases have equal relative selectivity's toward to the three isomers.

The para isomer displayed the longest retention times for both HP-1ms and HP-5ms columns and the *ortho* isomer gave the shortest retention times on both columns.

Fig. 1 shows the EI mass spectra for the three isomers. Classical mass spectral interpretation would predict initial ionization on the indole nitrogen or on the carbonyl oxygen. Because of the extended conjugation throughout the entire indole-carbonyl system, ionization anywhere within the indole-carbonyl system should result in similar fragmentation patterns, regardless of where the electron was initially abstracted. The product ion at *m*/*z* 214 can be described as formally originating from the nitrogen or from the carbonyl oxygen (Scheme 1 versus Scheme 2), but both mechanisms are essentially the same because the precursors and products of Schemes 1 and 2 are resonance structures. The *m*/*z* 214 base peak ion results from the loss of the methoxybenzyl or methylanisole radical, as shown in Schemes 1 and 2. In theses schemes, the bond between the carbonyl carbon and benzyl carbon (i.e. the alpha carbon) is homolytically cleaved, with one electron going into the indole-carbonyl system and the other electron forming the methoxybenzyl radical leaving group. Inductive cleavage of the same alpha carbon could also form the methoxybenzyl ion at *m*/*z* 91 instead of the methoxybenzyl radical, as discussed later.

Previous work has shown that MS/MS of the *m*/*z* 214 ion fragments into product ions at *m*/*z* 144, 116, and 89 ions [17]. The *m*/*z* 144 fragment may form by a 1,3 hydride transfer from the alkyl carbon beta to the nitrogen with concerted breaking of the σ bond between the nitrogen and the alkyl group, which forms a π-bond on the pentene leaving group (Scheme 3). This transfer is not a "sigmatropic change of order" as defined by Woodward and Hoffmann [18] as it is not the migration of a σ bond flanked by a π bond but rather a σ bond flanked by saturated carbons. Orbital plots from 6-31G** calculations of the *m*/*z* 214 ion indicate the hydride transfer can occur suprafacially because the sp^3-hybridized carbon alpha to the N atom can freely rotate for orbital orientation for the transfer.

Note that the resonance structure of the *m*/*z* 214 product ion in Scheme 2 places a positive charge on the nitrogen, thereby making it more attractive to nucleophilic attack than the resonance form actually shown in Scheme 3. Subsequent fragmentation of the *m*/*z* 144 ion to the *m*/*z* 116 ion likely results from simple loss of carbon monoxide. The product ion at *m*/*z* 89 can be shown to form either in a concerted manner, via the loss of C_3HNO from the *m*/*z* 144 product, or via sequential losses of CO and HCN from *m*/*z* 144 to give a charged benzyne (C_7H_5) fragment ion at *m*/*z* 89. The benzyne product at *m*/*z* 89 commonly accompanies tropylium ions (*m*/*z* 91) in electron ionization spectra of aromatics and especially indoles.

It is clear from the MS/MS data of Westphal et al. [17] that the *m*/*z* 91 fragment ion does not result from secondary fragmentation of the *m*/*z* 214 ion. However, there is significant evidence in the literature that the tropylium ion at *m*/*z* 91 can originate from the methyl anisole precursor at *m*/*z* 121 [19–21]. As discussed above, inductive cleavage adjacent to the ionized carbonyl group is one potential pathway to forming the methoxybenzyl fragment at *m*/*z* 121. Alternatively, this fragment can also be formed via radical-directed cleavage following ionization of the methoxybenzyl group. As shown in Scheme 4, the charged methoxy-benzyl fragment can rearrange to a stable methoxy-cycloheptatrienyl cation at *m*/*z* 121, or eject a formaldehyde neutral (CH_2O) and rearrange to form a stable tropylium ion at *m*/*z* 91, the relative kinetics of which are dependent on the positional isomer [19–21].

The *ortho* effect relates to the steric ease with which substituent groups *ortho* to one another on an aromatic ring may undergo cyclic rearrangements—such as hydride shifts—leading to small neutral losses, such as formaldehyde. It is well known that because of the *ortho* effect, *o*-methoxybenzyl radicals are more prone to the loss of formaldehyde (CH_2O) than either the *meta* or *para* isomers [22–24] and that the fragmentation patterns of n-substituted methyl phenol ethers (anisoles) are similarly sensitive to such regiochemistry

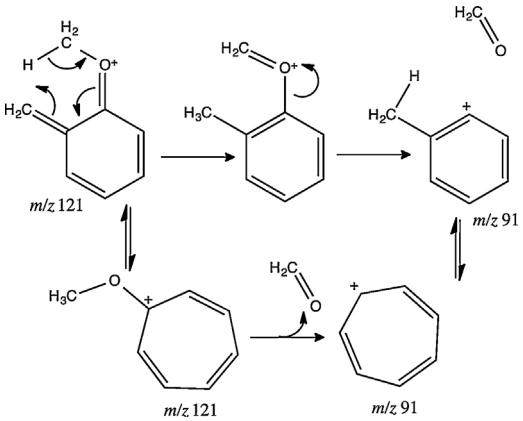

Scheme 4. Proposed scheme for producing the fragment at *m*/*z* 91 from the methyl anisole precursor at *m*/*z* 121. The top pathway requires an initial hydrogen transfer and is dependent on the relative position of the methyl group and methoxy groups, but the bottom pathway is independent of the methyl position.

Table 1
Comparison of sample means for peak abundances of selected ions normalized to *m*/*z* 214 (10,000). Cells with a gray background indicate significant differences between samples means, as determined by one-way ANOVA.

Sample	*m*/*z*				
	89	91	116	121	144
JWH-201					
Mean	151	58	423	402	1654
N	7	7	7	7	7
Std. deviation	49	20	82	89	198
JWH-250					
Mean	152	331	414	130	1646
N	14	14	14	14	14
Std. deviation	75	80	60	32	178
JWH-302					
Mean	168	147	462	187	1743
N	6	6	6	6	6
Std. deviation	66	60	110	45	247
Total					
Mean	155	219	427	213	1670
N	27	27	27	27	27
Std. deviation	65	137	78	127	195
One way ANOVA *F* value	0.128	45.85	0.807	59.07	0.526
Significance (α)	0.881	6×10^{-9}	0.458	5×10^{-10}	0.597

[24,25]. In an analogous study to the present article, the *ortho*-methoxy isomer of amphetamine analogs displays a much more dominant *m*/*z* 91 peak than the *meta* or *para* isomers [26]. Hydride transfers for substituents in the *meta* and *para* positions are much less likely to occur, if at all, because such shifts would require crossing the rigid pi system. The substituent groups of methoxybenzene may still influence the degree of hydride rearrangements (resulting in the loss of a neutral formaldehyde molecule), depending on the electron donating or withdrawing ability of the substituent and its position relative to the methoxy group [24].

Statistical analyses were performed to determine the significant differences between the abundances of the major fragment ions for the three positional isomers. EI spectra were collected on three different instruments over a period of weeks. Data from different instruments and different dates were pooled without bias. The results are shown in Table 1.

From the five largest peaks of interest, three peaks (*m*/*z* 89, *m*/*z* 116 and *m*/*z* 144) show no significant differences for the within-sample-variances and between-sample-variances. However, ions at *m*/*z* 91 and *m*/*z* 121 show very significant differences for the within-sample-variances and between-sample-variances, as indicated by the very small alpha values (6×10^{-9} and 5×10^{-10}, respectively). Post hoc analysis of the data using Tukey's LSD showed that the three conformers were significantly different at $p < 0.05$ for the relative abundance of the fragments at *m*/*z* 91 and *m*/*z* 121. None of the other fragments observed were significantly different between the three JWH conformers.

In this study, the mass spectra used were those obtained at the apex of the chromatographic peak for each isomer. Even if one uses spectra from the beginning or end of the chromatographic peak rather than the apex of the peak, changes in ratios due to mass spectral skewing (spectral tilting) should be minimal because (1) the mass difference between 91 and 121 is small and (2) the 91/121 ratio differences between the three compounds are significantly larger than the magnitude typically encountered from spectral tilting.

Principal component analysis (PCA) was also applied to the multivariate data set to assess the separation of the different samples (see Fig. 2). The suitability for PCA was confirmed through many correlation scores exceeding 0.3, a Kaiser–Meyer–Olkin sampling adequacy value of 0.65, and Bartlett's test of sphericity reaching statistical significance. The peak areas for *m*/*z* 214 were omitted because they are constant (10,000), by definition. The five remaining variables naturally reduced to two principal components with initial Eigenvalues exceeding 1. The correlation matrix in Table 2 shows strong anti-correlation between *m*/*z* 91 and *m*/*z* 121 with a value of −0.609. These two ions did not correlate very

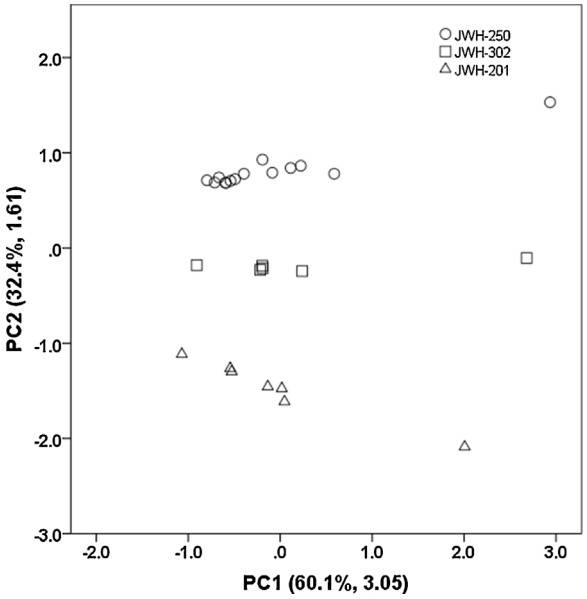

Fig. 2. A PCA plot to show the natural separation of the three JWH conformers based on the abundance of five fragment ions relative to *m*/*z* 214.

Table 2
Correlation matrix of the normalized peak areas for five different fragment ions normalized to *m*/*z* 214.

		89	91	116	121	144
Correlation	89	1				
	91	0.408	1			
	116	0.864	0.254	1		
	121	0.292	-0.609	0.373	1	
	144	0.879	0.308	0.956	0.344	1
Sig. (1-tailed)	89					
	91	0.017				
	116	0	0.101			
	121	0.07	0	0.028		
	144	0	0.059	0	0.039	

Table 3
A Component score coefficient matrix to show the loadings for the two principal components. *Extraction method*: Principal Component Analysis; *Rotation method*: Varimax with Kaiser Normalization.

	Component	
	1	2
89	0.312	0.05
91	0.119	0.558
116	0.317	−0.038
121	0.117	−0.55
144	0.32	−0.008

strongly with the other three ions, but the ions at *m*/*z* 89, *m*/*z* 116 and *m*/*z* 144 were strongly correlated with each other.

The PCA plot in Fig. 2 shows that the primary principal component (PC1) explained 60.1% of the variance and the second principal component (PC2) explained an additional 32.4% of the total variance. The combined components explained 92.5% of the total variance. The first principal component is ineffective at separating the three conformers, but the second component is clearly very effective, as demonstrated in the figure. The data points did not naturally separate by instrument or by date, which indicates that inter-instrument variability and data acquisition date have negligible effects relative to the effect of the positional isomer. The component score coefficient matrix provided in Table 3 shows that the fragments at *m*/*z* 89, *m*/*z* 116, and *m*/*z* 144 are weakly represented in PC2. However, *m*/*z* 91 has a strong positive loading and *m*/*z* 121 has a strong negative loading. Together, the separation of samples through PC2, the weak loadings for the three ions at *m*/*z* 89, *m*/*z* 116 and *m*/*z* 144, and the negative correlation between *m*/*z* 91 and *m*/*z* 121 indicate that these two ions alone provide most of the variance for distinguishing between sample types.

The anti-correlation of fragment ion abundances *m*/*z* 91 and *m*/*z* 121 are best expressed and compared as a ratio. The bar and whisker plot shown in Fig. 3 shows the effectiveness of such discrimination. The sample means are easily distinguished visually, but can also be compared statistically.

One-way ANOVA of the ratio of *m*/*z* 121:91 gave an F_{calc} value of 868 and a significant difference of $p = 4 \times 10^{-23}$ indicating that the

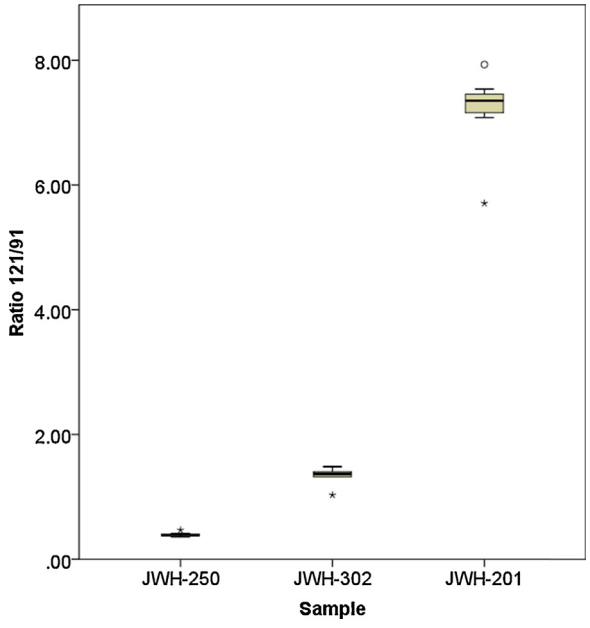

Fig. 3. Bar and whisker plot of the ion abundance ratio ion ratios *m*/*z* 121:91 to show the statistical difference between the three regioisomers of JWH. The circles and stars show outliers at $p < 0.05$.

Table 4
Comparison of ion ratios *m*/*z* 121:91 for synthetic cannabinoids JWH-250, JWH-302, JWH-201.

	JWH-250 (*N* = 17)	JWH-302 (*N* = 6)	JWH-201 (*N* = 7)
Mean ratio 121:91	0.40	1.3	7.2
95% CI	0.02	0.1	0.5

within-isomer variance is vastly smaller than the between-isomer variance. Post hoc analysis using Tukey's LSD showed that JWH-250 and JWH-302 were the least significantly different, but could still be distinguished with a confidence of $p = 1.7 \times 10^{-5}$ (Table 4).

4. Conclusions

Because the GC retention times are so similar, and because compound identification is so important in drug analysis and forensic toxicology, we conducted a thorough comparison of the fragmentation behavior of the three positional isomers of JWH-250. Analysis of the product ion abundances showed that the three isomers can in fact be distinguished, even though the fragmentation spectra are very similar at first glance. In a normally tuned electron ionization mass spectrometer at 70 eV, the average ion abundance ratios for *m*/*z* 121:91 are 0.4 for JWH-250, 1.3 for JWH-302, and 7.2 for JWH-201. These ratios were consistent across different weeks on the same instrument and across different GC-MS instruments. The differences in *m*/*z* 121:91 ratios can be explained by the relative positions of the methoxy group to the indole-carbonyl system and the relative propensity for losing the methoxy group as formaldehyde (CH_2O) from the aromatic ring. The ratio of these two fragments is qualitatively consistent with previous studies of substituted anisoles and substituted methylamphetamines and would be expected to be consistent in positional isomers of current and future synthetic drug analogs.

References

[1] V. Auwarter, S. Dresen, W. Weinmann, M. Muller, M. Putz, N. Ferreiros, 'Spice' and other herbal blends: harmless incense or cannabinoid designer drugs? J. Mass Spectrom. 44 (2009) 832–837.
[2] M.M. Aung, G. Griffin, J.W. Huffman, M.J. Wu, C. Keel, B. Yang, V.M. Showalter, M.E. Abood, B.R. Martin, Influence of the N-1 alkyl chain length of cannabimimetic indoles upon CB1 and CB2 receptor binding, Drug Alcohol Depend. 60 (2000) 133–140.
[3] J.W. Huffman, P.V. Szklennik, A. Almond, K. Bushell, D.E. Selley, H.J. He, M.P. Cassidy, J.L. Wiley, B.R. Martin, 1-Pentyl-3-phenylacetylindoles, a new class of cannabimimetic indoles, Bioorg. Med. Chem. Lett. 15 (2005) 4110–4113.
[4] L. Ernst, H.M. Schiebel, C. Theuring, R. Lindigkeit, T. Beuerle, Identification and characterization of JWH-122 used as new ingredient in Spice-like herbal incenses, Forensic Sci. Int. 208 (2011) E31–E35.
[5] R. Kikura-Hanajiri, N. Uchiyama, M. Kawamura, Y. Goda, Changes in the prevalence of synthetic cannabinoids and cathinone derivatives in Japan until early 2012, Forensic Toxicol. 31 (2013) 44–53.
[6] R. Heltsley, M.K. Shelby, D.J. Crouch, D.L. Black, T.A. Robert, L. Marshall, C.L. Bender, A.Z. DePriest, M.A. Colello, Prevalence of synthetic cannabinoids in US athletes: initial findings, J. Anal. Toxicol. 36 (2012) 588–593.
[7] K. Simolka, R. Lindigkeit, H.M. Schiebel, U. Papke, L. Ernst, T. Beuerle, Analysis of synthetic cannabinoids in spice-like herbal highs: snapshot of the German market in summer 2011, Anal. Bioanal. Chem. 404 (2012) 157–171.
[8] United Nations office of Drugs and Crime (UNODC), Synthetic Cannabinoids in Herbal Products, 2013, http://www.unodc.org/documents/scientific/Synthetic_Cannabinoids.pdf
[9] S. Dresen, S. Kneisel, W. Weinmann, R. Zimmermann, V. Auwarter, Development and validation of a liquid chromatography-tandem mass spectrometry method for the quantitation of synthetic cannabinoids of the aminoalkylindole type and methanandamide in serum and its application to forensic samples, J. Mass Spectrom. 46 (2011) 163–171.
[10] S. Dresen, N. Ferreiros, M. Putz, F. Westphal, R. Zimmermann, V. Auwarter, Monitoring of herbal mixtures potentially containing synthetic cannabinoids as psychoactive compounds, J. Mass Spectrom. 45 (2010) 1186–1194.
[11] S. Kneisel, V. Auwarter, Analysis of 30 synthetic cannabinoids in serum by liquid chromatography–electrospray ionization tandem mass spectrometry after liquid–liquid extraction, J. Mass Spectrom. 47 (2012) 825–835.

[12] S. Kneisel, F. Westphal, P. Bisel, V. Brecht, S. Broecker, V. Auwarter, Identification and structural characterization of the synthetic cannabinoid 3-(1-adamantoyl)-1-pentylindole as an additive in herbal incense, J. Mass Spectrom. 47 (2012) 195–200.
[13] D. Harris, S. Hokanson, V. Miller, GC–MS differentiation of three synthetic cannabinoid positional isomers: JWH-250, JWH-302, and JWH-201, J. Clan. Lab. Invest. Chem. Assoc. 21 (2011) 20–29.
[14] V. Shevyrin, V. Melkozerov, A. Nevero, O. Eltsov, Y. Shafran, Analytical characterization of some synthetic cannabinoids, derivatives of indole-3-carboxylic acid, Forensic Sci. Int. 232 (2013) 1–10.
[15] W.H. Soine, W. Duncan, R. Lambert, R. Middleberg, H. Finley, D.J. O'Neil, Differentiation of side-chain isomers of ring-substituted amphetamines using gas chromatography infrared mass spectrometry (GC/IR/MS), J. Forensic Sci. 37 (1992) 513–527.
[16] J.F. Casale, P.A. Hays, Characterization of eleven 2,5-dimethoxy-N-(2-methoxybenzyl)phenethylamine (NBOMe) derivatives and differentiation from their 3- and 4-methoxybenzyl analogues: part I, Microgram J. 9 (2012) 84–109.
[17] F. Westphal, T. Junge, F. Sönnichsen, P. Rösner, J. Schäper, Ein neuer wirkstoff in SPICE-artigen Kräutermischungen: Charakterisierung von JWH-250, seinen methyl- und trimethylsilylderivaten, Toxichem. Krimtech. 77 (2010) 8–22.
[18] R. Woodward, R. Hoffman, The Conservation of Orbital Symmetry, Verlag Chemie Gmblt Academic Press, 1970.
[19] J. Brodbelt, C.C. Liou, T. Donovan, Selective adduct formation by dimethyl ether chemical ionization in a quadrupole ion trap mass-spectrometer and a conventional ion-source, Anal. Chem. 63 (1991) 1205–1209.
[20] R.G. Cooks, M. Bertrand, J.H. Beynon, M.E. Rennekam, D.W. Setser, Energy partitioning data as an ion structure probe: substituted anisoles, J. Am. Chem. Soc. 95 (1973) 1732–1739.
[21] F. Meyer, A.G. Harrison, An electron impact study of methyl phenyl ethers, Can. J. Chem. 42 (1964) 2008–2017.
[22] Z. Pelah, H. Budzikiewicz, M. Ohashi, J.M. Wilson, C. Djerassi, Mass spectrometry in structural and stereochemical problems. 34. Aromatic methyl and ethyl ethers, Tetrahedron 19 (1963) 2233.
[23] C. Barnes, J. Occolowitz, The mass spectra of phenyl methyl ethers, Aust. J. Chem. 16 (1963) 219–224.
[24] F.W. McLafferty, M.M. Bursey, Substituent effects in unimolecular ion decompositions. VIII. Rearrangement ions in the mass spectra of substituted phenyl methyl ethers, J. Org. Chem. 33 (1968) 124–127.
[25] T. Awad, J. DeRuiter, C.R. Clark, Gas chromatography–mass spectrometry analysis of regioisomeric ring substituted methoxy methyl phenylacetones, J. Chromatogr. Sci. 45 (2007) 458–465.
[26] D. Blachut, W. Danikiewicz, M. Olejnik, Z. Czarnocki, Electron ionization mass spectrometry as a tool for the investigation of the ortho effect in fragmentation of some Schiff bases derived from amphetamine analogs, J. Mass Spectrom. 39 (2004) 966–972.